THE
PHYSICAL REVIEW

A journal of experimental and theoretical physics established by E. L. Nichols in 1893

SECOND SERIES, VOL. 164, NO. 2 10 DECEMBER 1967

Interaction of Microwave Phonons with Iron-Group Ions Fe^{2+} and Ni^{2+} in Magnesium Oxide

M. F. LEWIS

The General Electric Company, Limited, Central Research Laboratories, Hirst Research Centre, Wembley, England

AND

A. M. STONEHAM

Theoretical Physics Division, Atomic Energy Research Establishment, Harwell, Berkshire, England

(Received 7 June 1967)

Experiments which study the spin-lattice interactions of Fe^{2+} and Ni^{2+} in MgO are reported. These are acoustic saturation and the measurement of spin-lattice relaxation rates and the shapes of strain-broadened spin-resonance lines.

The acoustic saturation behavior in $MgO:Fe^{2+}$ follows the predicted behavior quite well, but is complicated by a large background, probably due to mode conversion. The two spin-lattice relaxation times of $MgO:Fe^{2+}$ agree well with theory in magnitude and in their dependence on the magnetic field orientation and the position in the inhomogeneous line at which they are measured. The spin-lattice rate of Ni^{2+} is in rather poor agreement with theory, probably because of impurities.

The acoustic saturation has been exploited to measure the broad line shapes accurately, and the Fe^{2+} line *shape* is found to vary with magnetic field orientation. This is in accord with theory. If the various ions experience the same internal strain distributions, the linewidths imply $|G_{11}(Fe^{2+})/G_{11}(Ni^{2+})| = 10.0 \pm 0.2$ and $|G_{44}(Fe^{2+})/G_{44}(Ni^{2+})| = 7.8 \pm 0.8$. If the Fe^{2+} relaxation is purely by the direct process and if the MgO phonon system is reasonably isotropic, the anisotropy of this relaxation rate gives $|G_{11}(Fe^{2+})/G_{44}(Fe^{2+})| = 1.59 \pm 0.09$. With these qualifications, the ratios are considerably more accurate than direct measurements of the G_{ij}.

1. INTRODUCTION

THE interaction of microwave phonons with paramagnetic centers in solids has been a fruitful area of research since the development of methods for generating ultrasonics with frequencies of order 10^{10} cps. Such studies can give unambiguous information on the mechanism and strength of the interaction and can supplement the results of the more conventional magnetic resonance and relaxation work. Two techniques are important. The first measures the attenuation of phonons incident on magnetic centers resonant with the phonons.[1–10] With present techniques, attenuation experiments are only possible in systems with strong spin-lattice coupling or systems with an undesirably high concentration of paramagnetic centers. The second method measures the saturation of the spin system by an ultrasonic field.[11–18] This has, in principle, much wider application, but suffers from the disadvantage that spurious effects can mask the par-

[1] E. B. Tucker, Phys. Rev. Letters **6**, 183 (1961).
[2] E. B. Tucker, Phys. Rev. Letters **6**, 547 (1961).
[3] N. S. Shiren, Phys. Rev. **128**, 2103 (1962).
[4] D. I. Bolef and R. B. Gosser, Proc. Phys. Soc. (London) **79**, 442 (1962).
[5] W. I. Dobrov and M. E. Browne, in *Paramagnetic Resonance*, edited by W. Low (Academic Press Inc., New York, 1963), Vol. II, p. 447.
[6] W. I. Dobrov and M. E. Browne, in *Proceedings of the Eleventh Colloque Ampere, Eindhoven* (North-Holland Publishing Company, Amsterdam, 1962).
[7] N. S. Shiren, Phys. Rev. Letters **11**, 3 (1963).
[8] W. I. Dobrov, Phys. Rev. **134**, A734 (1964).
[9] G. C. Wetsel and P. L. Donoho, Phys. Rev. **139**, A334 (1965).
[10] J. R. Fletcher, F. G. Marshall, V. W. Rampton, P. M. Rowell, and K. W. H. Stevens, Proc. Phys. Soc. (London) **88**, 127 (1966).
[11] E. H. Jacobsen, N. S. Shiren, and E. B. Tucker, Phys. Rev. Letters **3**, 81 (1959).
[12] N. S. Shiren and E. B. Tucker, Phys. Rev. Letters **6**, 105 (1961).
[13] P. H. Carr and M. W. P. Strandberg, J. Phys. Chem. Solids **23**, 923 (1962).
[14] N. S. Shiren, in *Paramagnetic Resonance*, edited by W. Low (Academic Press Inc., New York, 1963), Vol. II, p. 482.
[15] G. W. Farnell and A. L. Taylor, Can. J. Phys. **42**, 595 (1964).
[16] M. F. Lewis, Phys. Letters **17**, 183 (1965).
[17] M. F. Lewis, Phys. Letters **19**, 459 (1965).
[18] M. F. Lewis, H. M. Rosenberg, and J. K. Wigmore, Phys. Status Solidi **15**, 317 (1966).

ticular interaction of interest. The saturation method is used here, in conjunction with conventional magnetic resonance and relaxation techniques.

The system MgO:Fe^{2+} has been studied extensively by ultrasonic methods.[3,4,7,14,16,17,19–26] Its strong spin-phonon coupling permits easy observation of ultrasonic attenuation and dispersion on magnetic resonance and of the paramagnetic saturation by microsecond ultrasonic pulses. The experiments to be described are largely concerned with paramagnetic saturation, and some have been briefly reported before.[16,17] The ultrasonic work is supplemented by more conventional spin-resonance and relaxation work. The saturation experiments use simultaneous ultrasonic and conventional paramagnetic resonance arrangements. This method can detect microwave ultrasonic energy—the measurement is not sensitive to the shape of the ultrasonic wavefront, in contrast to the conventional piezoelectric detection methods.

Two systems are discussed in this article: MgO:Fe^{2+} and MgO:Ni^{2+}. These ions have threefold degenerate ground states in a strictly cubic field. Their effective spin Hamiltonians are

$$\mathcal{H}=g\beta\mathbf{H}\cdot\mathbf{S}' \qquad (1)$$

where $S'=1$ and $g=3.4277$ for Fe^{2+}, $g=2.227$ for Ni^{2+}.[27] Both have a strong spin-lattice coupling and both have resonance lines greatly broadened by microscopic strains in the MgO lattice. These local departures from cubic symmetry add a term

$$\mathcal{H}_1=\mathbf{S}\cdot\mathbf{D}\cdot\mathbf{S} \qquad (2)$$

to $\mathcal{H}$, which splits the $S_z=\pm1$ levels from the $S_z=0$ level. If we neglect second-order effects, then for any form of strain the $S_z'=\pm1$ levels are degenerate in a zero magnetic field. Changes in the g tensor from local strains are usually negligible. The energy levels are shown later in Fig. 7.

The spin-resonance spectrum consists of a broad $\Delta M=1$ line, a sharp double quantum line superimposed on the center of the $\Delta M=1$ line, and a $\Delta M=2$ line. We have studied the spin-resonance line shapes, spin-lattice-relaxation times, and ultrasonic attenuation of both systems as a function of the orientation of the applied magnetic field. The ultrasonic saturation technique has enabled us to measure the line shapes of MgO:Fe^{2+} with great accuracy—in particular the usual difficulty in fixing the base line of a wide resonance line does not arise. The accuracy of these measurements (described in detail in Sec. 6) permits a comparison of the $\Delta M=1$ line shape as a function of the magnetic field orientation. The small angular variation obtained appears to be consistent with Stoneham's theory of broadening by dislocations.[28] Other lines, including the Ni^{2+} lines, have been studied using conventional electron-spin-resonance techniques. From these linewidths we can compare the spin-lattice coupling coefficients of Fe^{2+} and Ni^{2+} under the assumption that the magnetic ions in any one crystal experience an average distribution of strains which is the same for all species. The ratios of the coupling coefficients are (subject to this assumption) more accurately determined than by the usual static-stress experiments, and our data can be used to improve the consistency of the results at present in the literature.

The spin-lattice relaxation times (t_1) of both Fe^{2+} and Ni^{2+} in MgO have been measured as a function of temperature, magnetic field orientation, and position in the $\Delta M=1$ resonance line. Relaxation proceeds by the direct process at the temperatures studied (1.8 to 7°K). As both Fe^{2+} and Ni^{2+} have ground states with three levels, the recovery is characterized by two relaxation times. By measuring the relaxation time at different positions in the resonance line, it turns out that we can separate these times rather well. The results are analyzed in Sec. 4. For MgO:Fe^{2+} the rate and its angular dependence is in good accord with theory for both these relaxation times. The agreement is less successful for MgO:Ni^{2+}, although the reasons for this are not obvious.

Regrettably, these experiments only deal with a small number of systems—MgO:Fe^{2+} and MgO:Ni^{2+}. They do, however, give much information on the microscopic strains in the host lattice and on the spin-lattice interaction.

2. EXPERIMENTAL APPARATUS AND TECHNIQUES

The apparatus is shown in Fig. 1. Basically it consists of two parts. One is a 2J51A pulsed magnetron, tuneable reentrant cavity, and 1 in. long, $\frac{1}{8}$-in.-diam x-cut quartz transducer for the generation and detection of longitudinal microwave phonons.[29] The echoes are observed in reflection using superheterodyne receiver 1 (bandwidth 5 Mc/sec) and the cathode-ray oscilloscope. The other half of the apparatus is a tuneable ESR spectrometer operating in the same frequency range as the ultrasonic cavity, viz, 9155± 200 Mc/sec. The bandwidth of the ESR receiver is ~5 Mc/sec to permit observation of transient signals

[19] N. S. Shiren, Phys. Rev. Letters **6**, 168 (1961).
[20] V. W. Rampton and P. M. Rowell, Phys. Letters **7**, 12 (1963).
[21] N. S. Shiren, Appl. Phys. Letters **4**, 82 (1964).
[22] R. Guermeur, J. Joffrin, A. Levelut, and J. Penne, Phys. Letters **13**, 107 (1964).
[23] R. Guermeur, J. Joffrin, A. Levelut, and J. Penne, Phys. Letters **15**, 203 (1965).
[24] R. Guermeur, J. Joffrin, A. Levelut, and J. Penne, Compt. Rend. Acad. Sci. (Paris) **260**, 108 (1965).
[25] I. S. Ciccarello, A. Arzt, and K. Dransfeld, Phys. Rev. **138**, A934 (1965).
[26] N. S. Shiren, in *Proceedings of the XIth Colloque Ampere, Eindhoven* (North-Holland Publishing Company, Amsterdam, 1962), p. 114.
[27] W. Low, in *Paramagnetic Resonance in Solids*, edited by F. Seitz and D. Turnbull (Academic Press Inc., New York, 1960).
[28] A. M. Stoneham, Proc. Phys. Soc. (London) **89**, 909 (1966).
[29] H. E. Bommel and K. Dransfeld, Phys. Rev. Letters **1**, 234 (1958).

with rise times of ~1 μsec. The signal klystron can be locked to the transmission cavity by means of 500-kc/sec. frequency modulation and phase-sensitive detection.[30] A metal tube surrounds the quartz rod and forms a cut-off waveguide to prevent microwave leakage between the cavities. The [001]-cut MgO crystal is about 8 mm long and is situated in the uniform (vertical) microwave magnetic field of the ESR cavity operating in the H_{102} mode, and is aligned so that the external magnetic field swings in the (horizontal) $(1\bar{1}0)$ plane through the principal symmetry axes [001], [111], and [110].

The ultrasonic bond between the optically polished faces of the MgO and quartz rod is made with "Araldite" in the following manner. A minute spot of "Araldite" is placed on one face, and the two crystals are wrung together. The parallelism of the bond is tested by observing the wedge fringes between the two faces using white light, and the two crystals are twisted together until the fringe pattern shows the faces are most nearly parallel. In this way the variation in the thickness of the bond can be made rather less than an optical wavelength. The Araldite is sufficiently viscous to maintain this position during setting. The bonds, which can be used repeatedly, have a power efficiency of about 10%; this was estimated from the piezoelectrically detected echo patterns of some fifty bonds between quartz transducers and SiO_2, MgO, $MgAl_2O_4$, Si, GaAs, and yttrium iron garnet (YIG). We believe that the figure of 10% for the bond efficiency

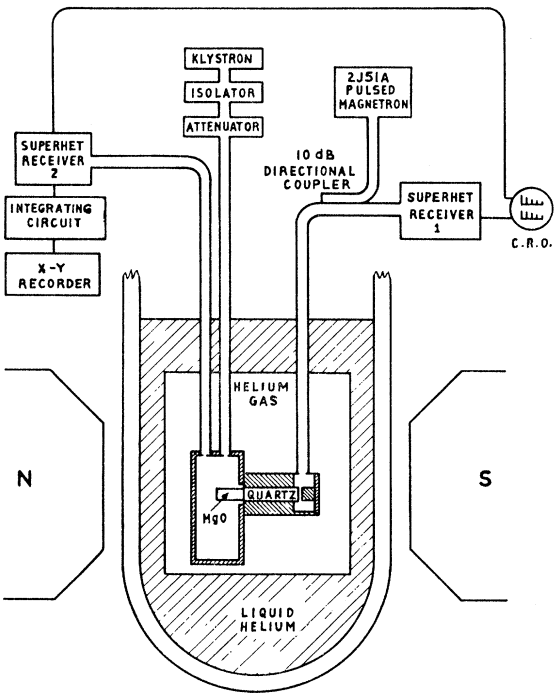

FIG. 1. Schematic diagram of the apparatus.

[30] R. V. Pound, Rev. Sci. Instr. **17**, 490 (1946).

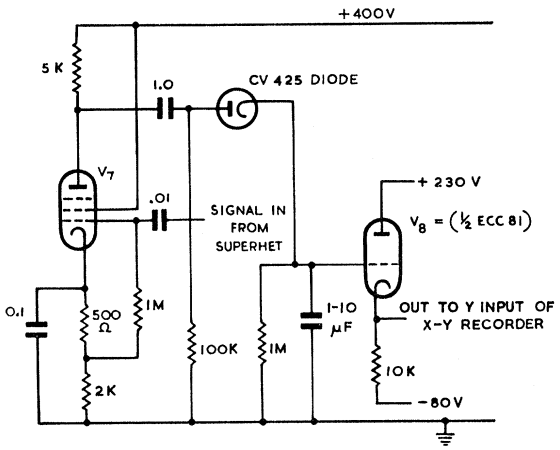

FIG. 2. Gating circuit and pulse integrator used to improve the signal: noise ratio of the piezoelectric echo pattern and transient ESR signals.

is probably accurate to a factor of 3. We have had no success in producing bonds for transversely polarized microwave ultrasound, presumably because of the high attenuation in amorphous materials.[31]

During experiments we monitor both the piezoelectric echo pattern and the microwave power transmitted through the ESR cavity. The latter changes rapidly in the presence of an ultrasonic pulse due to saturation of the spin system, as discussed later. To improve the signal/noise ratio of both the piezoelectric echo pattern and the transient signal from the ESR spectrometer, we have used a simple gating circuit and pulse integrator. The majority of this circuit is given in Ref. 32. To this we have added the section shown in Fig. 2. The output of the integrating circuit is fed to the Y input of an X-Y recorder. For recording the piezoelectric echo pattern, the X-input of the X-Y recorder is driven from the slowly swept voltage which controls the separation of the gate and the trigger pulse (this is the voltage of the wiper of the 250 kΩ potentiometer in Ref. 32).

In measuring spin-lattice relaxation times the attenuated magnetron output is injected into the ESR klystron line and the receiver 2 is protected with a fast semiconductor switch. The integrator circuit described above can also be used to improve the signal/noise ratio of the recovering ESR signal. For monitoring the ESR signal or an individual echo as a function of magnetic field the X input is driven from the voltage across the magnet; for monitoring as a function of the magnetic field orientation it is driven from a helipot circuit attached to the rotating base of the magnet. The gate width is usually set at 1 μsec, which is the duration of an ultrasonic pulse. With a pulse repetition frequency of 1000/sec and a final time constant of 1 sec the

[31] P. G. Klemens, Proc. Roy. Soc. (London) **A208**, 108 (1951).
[32] F. J. M. Farley, *Elements of Pulse Circuits* (Methuen Monographs, London, 1964), Chap. 7, p. 115.

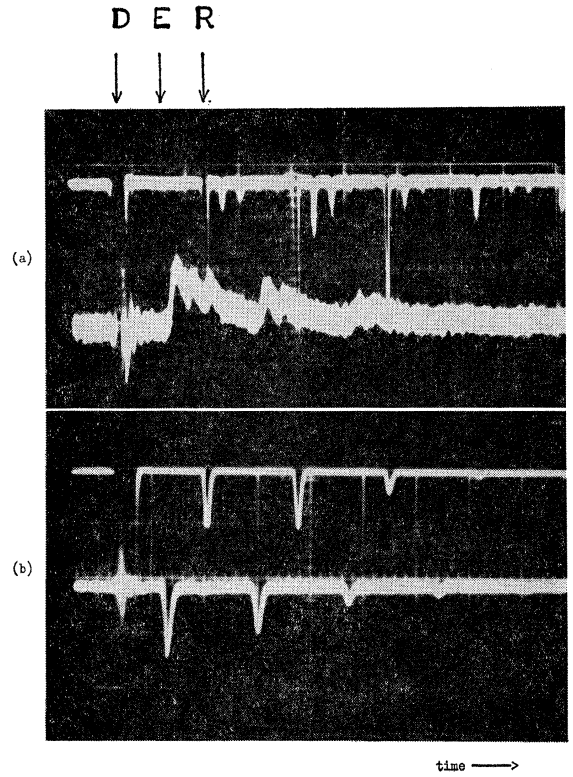

FIG. 3. Echo patterns detected piezoelectrically (upper traces) and saturation signals (lower traces) at 4.2°K. The large scale divisions of the time base are 5 μsec apart. *D* is the driving pulse, *E* the point at which the phonon pulse enters the MgO, and *R* the first reflection from the MgO: quartz bond. (a) MgO with about 100 ppm Fe^{2+}; only about one-third of the MgO specimen is in the ESR cavity. (b) MgO with about 3000 ppm Fe^{2+}. All the specimen is in the ESR cavity. The opposite signs of the lower (saturation) traces in (a) and (b) are of no significance. The first echo of the lower trace in (b) is slightly reduced by electronic effects.

theoretical gain in signal/noise ratio is $(1000)^{1/2}$; in practice, because of imperfect components, a gain of ten times is realized. This was invaluable in the experiments reported here.

3. EXPERIMENTAL OBSERVATIONS

One of the original aims of the experiments reported here was to induce phonon-photon double quantum transitions between the $S_z'=+1$ and $S_z'=-1$ levels. Such transitions were observed by Shiren.[19] We were unable to observe this effect, but were able to observe saturation of the $\Delta M=1$ and $\Delta M=2$ lines by the microwave phonons. Since the signals observed in the two cases are rather similar it is necessary to justify our interpretation. The major difference is that the signals observed in the two experiments are opposite in sign. In the double quantum experiment there is an *additional* microwave absorption in the presence of the phonons, whereas ultrasonic saturation of the spin system *reduces* the ESR microwave absorption. The sign of the signal shows that we are observing *saturation* of the spin system. This can be verified in other ways. Thus in our work the phonon and photon energies were essentially equal and their sum was not, in general, equal to the $\Delta M=2$ transition energy. The saturation was observed over a wide range of magnetic fields. Further the microwave photon power level used was much lower in our experiments. An example of the signal observed has been given in Ref. 16. In Fig. 3(a) we show the signal observed for MgO containing 100 ppm of Fe^{2+}. Only about one-third of the MgO crystal is situated in the ESR cavity. The effects of successive phonon reflections are observed in both the MgO crystal (round-trip time ~1.7 μsec) and the quartz crystal (round-trip time ~8.9 μsec). The saturation rises rapidly after about 4.5 μsec, as soon as the phonon pulse reaches the MgO monitored by spin resonance. The rise time observed is limited by the response time of the receiver and by the transit time through the MgO; the recovery time is longer, of order 10 μsec. In a heavily doped specimen (estimated to contain 3000 ppm Fe^{2+}) the relaxation time is greatly reduced, probably by cross relaxation to fast relaxing centers. The signal obtained [Fig. 3(b)] shows that the saturation recovers much more rapidly than in the dilute sample; here the observed recovery time may be as short as the response time of the receiver. The saturation is observed for perhaps 1 μsec, which is of the order of the pulse duration. In this specimen echoes were only detected piezoelectrically when the applied field exceeded ~3000 Oe.

The spin system is only partially saturated at low phonon powers. The variation of the signal with magnetic field orientation then measures the product of the spin-phonon transition probability W and the spin-lattice relaxation time t_1. To extract W and its dependence on the magnetic field direction the angular

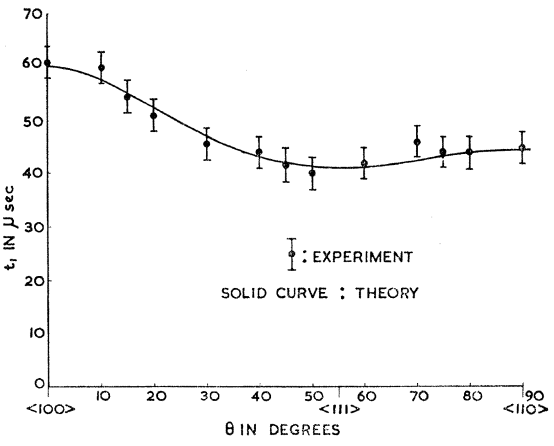

FIG. 4. The dependence of the Fe^{2+} relaxation time on magnetic field orientation. The full curve is a least-squares fit of the data to a relation

$$t_1=[A+B(l^4+m^4+n^4)]^{-1},$$

where the direction cosines of the field with respect to the crystal axes are (l, m, n).

dependence of t_1 must be measured separately. This has been done using the pulse-saturation recovery technique.[33] Some of the results are presented in Fig. 4, where the measurements shown were made with the magnetic field set about 20 Oe from the center of the $\Delta M=1$ line. These results are discussed in detail in Sec. 4.

At the highest phonon powers both the saturated ESR signal and the ultrasonic attenuation (measured piezoelectrically) flatten off, (see also Ref. 3); the spin system is clearly highly saturated. In these circumstances the ESR signal is a measure of the intensity of the resonance absorption line. The line shapes have been traced out using a swept magnetic field and the monitoring circuit of Fig. 2. These are shown in Fig. 5 for various magnetic field orientations, all being drawn on the same scale. The *line shape* changes with the magnetic field orientation. For an [001] field, Fig. 5(a) shows that the line shape is remarkably closely Lorentzian. Slight departures (about the thickness of the trace) are observed for H along the [110] axis. These become more marked until quite distinct departures from Lorentzian towards Gaussian are seen with H in the [111] direction. Finally, in Fig. 5(d) we show a tracing of the height of the ultrasonic echo taken at low phonon powers. This was taken with H roughly along the [111] axis and enables us to compare the phonon and photon line shapes. These detailed measurements of line shape would not have been possible with conventional ESR techniques (e.g., using field modulation and phase-sensitive detection) as any zero-field absorption introduces an uncertainty in the base line location which rules out detailed measurements of the line shape.

The $\Delta M=1$ and $\Delta M=2$ lines are inhomogeneously broadened, the homogeneous broadening being of order 2 Oe (~10 Mc/sec). The homogeneous contribution is needed in Sec. 6. This can be estimated from the measurable dipolar broadening of other lines (e.g., Fe^{3+}) and by measuring the signal at low powers as a function of the difference between the phonon and microwave frequencies. Khutsishvili[34] has recently discussed the relation between the line shape obtained in the latter class of experiment and the spin packet line shape. Our experiment differs slightly from the one he discusses in that the spin-phonon line shape and the spin-photon line shape are different. This affects the detailed discussion, but the general features are unaltered. Khutsishvili's work shows that in an experiment such as ours the line shape as a function of the difference in phonon and photon frequencies is related to the spin packet line shape. The relation is not simple, but depends on the degree of saturation induced by the phonons. The widths of the spin packet line shape and the observed shape are, however, of the same order of magnitude over an appreciable range of saturations. As we have not made measurements over a wide range of saturation the results we quote are simply of the order of the spin packet widths. For a specimen containing ~200 ppm Fe^{2+}, ~55 ppm Fe^{3+}, ~20 ppm Cr^{3+}, and ~20 ppm Mn^{2+} the average results are

$$\Delta M=1 \text{ line}, \quad \Delta\nu=7\pm2 \text{ Mc/sec},$$
$$\Delta M=2 \text{ line}, \quad \Delta\nu=10\pm2 \text{ Mc/sec},$$

where $\Delta\nu$ is the separation of the half-power points. Some confirmation of these values is provided by direct calculation. For most purposes we want the microwave *photon* linewidth, rather than the spin-phonon linewidth estimated in the Appendix of Ref. 3. The Kittel-

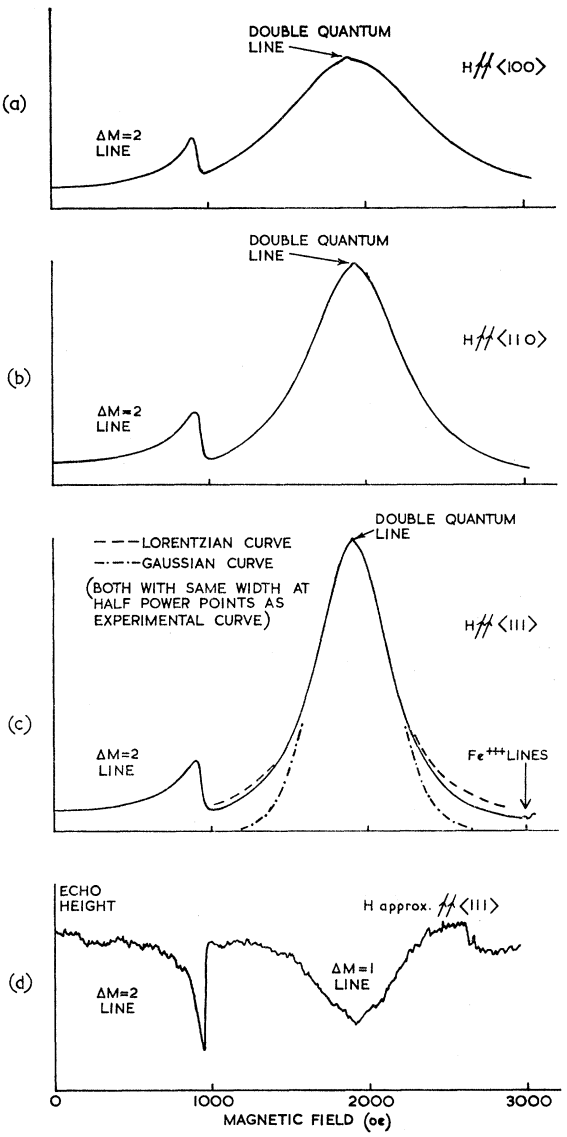

FIG. 5. (a), (b), and (c) give the spin-photon line shapes, measured by the saturation method, for different magnetic field orientations. (d) gives the spin-phonon line shape measured by the piezoelectrically detected echo height.

[33] J. A. Giordmaine, L. E. Alsop, F. R. Nash, and C. H. Townes, Phys. Rev. **109**, 302 (1958).

[34] G. R. Khutsishvili, Zh. Eksperim. i Teor Fiz. **50**, 1641 (1966) [English transl.: Soviet Phys.—JETP **23**, 1092 (1966)].

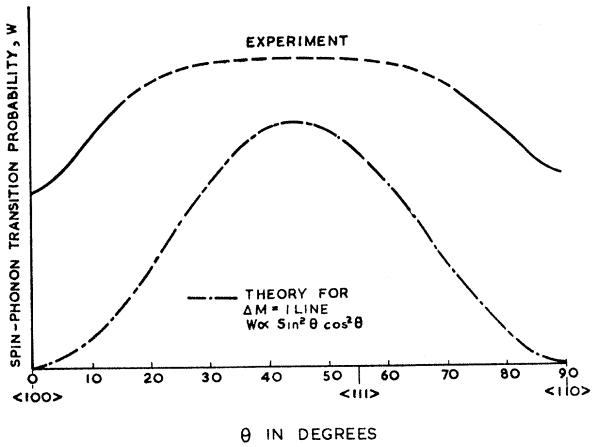

FIG. 6. The spin-phonon transition probability W_p as a function of magnetic field orientation.

Abrahams method[35] is directly applicable, although we must make a minor change because the magnetic impurities in MgO lie on a face-centered-cubic lattice. The $\Delta M=1$ line in the specimen cited has a predicted dipolar width of (6.5±3) Mc/sec, confirming the other estimates.

We return to the problem of saturation in Sec. 5 and are able to show that the degree of saturation achieved and the rise times observed are consistent with estimates of the ultrasonic power level. We also discuss reasons for the discrepancy in Fig. 6 between the experimental and theoretical curves of the angular dependence of the spin phonon transition probability. The line shapes of the various resonances are discussed in detail in Sec. 6.

4. SPIN-LATTICE RELAXATION TIMES

In this section we discuss the relaxation times and compare them with theory. The main effect of the random strains in the lattice on the Fe^{2+} and Ni^{2+} is to move the $M_z=0$ level with respect to the center of 7(a). In Fig. 7(b) we show the direct process spin-lattice transitions and their probabilities. The transitions shown are in all cases those for phonon absorption; the corresponding phonon emission and absorption probabilities ($\tilde{W}_i$ and W_i, respectively) are related

$$\tilde{W}_i/W_i=[n(E_i)+1]/n(E_i)=\exp(E_i/kT),$$

where E_i is the transition energy and $n(E_i)$ the corresponding Bose-Einstein occupation number (see, for example, Ref. 36).

Three level systems, such as Fe^{2+} and Ni^{2+}, have two spin-lattice relaxation times. We now relate these to the transition probabilities W_i. When the populations of the various spin levels are disturbed we may describe their recovery by rate equations, from which characteristic relaxation times can be obtained. If n_i is the deviation from equilibrium of the number of spins per unit volume in state $S_z=i$ these equations are

$$\begin{aligned}\dot{n}_1&=-n_1(\tilde{W}_2+\tilde{W}_3)+n_0W_2+n_{-1}W_3,\\ \dot{n}_0&=+n_1\tilde{W}_2-n_0(\tilde{W}_1+W_2)+n_{-1}W_1,\\ \dot{n}_{-1}&=+n_1\tilde{W}_3+n_0\tilde{W}_1-n_{-1}(W_3+W_1).\end{aligned}\tag{3}$$

When we concentrate on the spins relatively close to the center of the resonance line, for which $E_0-\frac{1}{2}(E_1+E_{-1})$ is less than, say, $\hbar\omega_0/10$, it is reasonable to assume that $W_1=W_2$. This is valid for most of the experiments to be described. Outside this regime the relaxation times have a complicated form which is consistent with the predictions given in general in Ref. 37. One further simplification is that at the temperatures of interest (2 to 7°K) $\hbar\omega_0/kT$ is only about 0.1 and we may assume

$$\tilde{W}_i=W_i$$

without significant error. With these simplifications we find

$$\begin{aligned}d(n_1-n_{-1})/dt&=-(W_1+2W_3)(n_1-n_{-1}),\\ d(n_0-\tfrac{1}{2}[n_1+n_{-1}])/dt&=-3W_1(\eta_0-\tfrac{1}{2}[n_1+n_{-1}]).\end{aligned}\tag{4}$$

Thus we expect the recovery to equilibrium to show two time constants, $\tau_a=1/(W_1+2W_3)$ characterizing the recovery of (n_1-n_{-1}), and a longer constant, $\tau_b=1/3W_1$, characteristic of the recovery of $n_0-\frac{1}{2}[n_1+n_{-1}]$. The relative importance of τ_a and τ_b depends on the particular way in which the spin populations have been disturbed; indeed, by suitably disturbing the populations we may measure both τ_a and τ_b.

The relaxation times have been measured by the pulse-saturation recovery technique. If the initial saturating pulse is applied at the peak of the resonance line, the spins which are saturated are those for which $E_1-E_0\simeq E_0-E_{-1}\simeq\hbar\omega_0$. Transitions from the levels $S_z=-1$ to $S_z=0$ and from $S_z=0$ to $S_z=+1$ are both induced, with the over-all result that (n_1-n_{-1}) is altered, but $n_0-\frac{1}{2}(n_1+n_{-1})$ is hardly affected. Thus for saturation exactly at $\hbar\omega_0$ we expect to measure τ_a only; τ_b will not be important. On the other hand, if the saturating pulse is applied slightly off resonance,

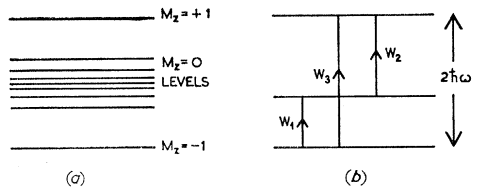

FIG. 7. (a) The energy levels of Fe^{2+} or Ni^{2+} in MgO, showing the effect of random strains. (b) The probabilities of transitions induced by thermal phonons. Only transitions in which one phonon is absorbed are shown.

[35] C. Kittel and E. Abrahams, Phys. Rev. **90**, 238 (1953).
[36] A. Abragam, *The Principles of Nuclear Magnetism* (Oxford University Press, London, 1961), pp. 267, 268.
[37] D. K. Ray, T. Ray, and P. Rudra, Proc. Phys. Soc. (London) **87**, 485 (1966).

at a frequency ω where

$$|\omega-\omega_0| \gg \text{spin packet width}, \quad (5)$$

the situation is less simple. In our experiments, the ratio (5) was about 10:1. Two groups of spins are affected, one for which $E_0-E_1\simeq\hbar\omega$ (so $E_1-E_0\neq\hbar\omega$) and the other for which $E_1-E_0\simeq\hbar\omega$. In the first group, the populations of the $S_z=0$ and $S_z=-1$ levels alone are appreciably changed, and in the second group those of the $S_z=0$ and $S_z=1$ levels alone. Thus both (n_1-n_{-1}) and $n_0-\frac{1}{2}(n_1+n_{-1})$ are altered for each group of spins and the recovery will be characterized by both τ_a and τ_b. As τ_b is the longer of the two times ($\tau_b\simeq 6\tau_a$) if the final stage of the recovery is monitored, τ_b will be obtained. We have neglected the spectral diffusion of energy across the resonance line in our discussion. This would give a temperature-independent contribution to the relaxation rate. This has not been observed. Measurements of the relaxation rate as a function of temperature have been reported.[38] The rate is proportional to the temperature in the range 2 to 7°K, as expected for a direct process.

The W_i and the relaxation times are now calculated explicitly in terms of the spin-lattice coupling coefficients and the properties of the host lattice. Ray *et al.*[37] have shown that the relaxation times, including their angular dependence, can be written in the general form[39]

$$\tau_a^{-1}=\tfrac{5}{3}Y_E+4Y_T+\Lambda(Y_E-Y_T),$$
$$\tau_b^{-1}=Y_E-\Lambda(Y_E-Y_T), \quad (6)$$

in which $\Lambda=l^4+m^4+n^4$ where the magnetic field has direction cosines (l, m, n) with respect to the cubic crystal axes. These results assume that the phonon system has cubic symmetry. If we assume an isotropic Debye model for the MgO lattice we find (either directly, or by comparison with the work of Shiren[26])

$$Y_E=[(\hbar\omega_0)^2kT/\pi\hbar^4\rho v^5]\tfrac{9}{16}G_{11}^2,$$
$$Y_T=[(\hbar\omega_0)^2kT/\pi\hbar^4\rho v^5]G_{44}^2, \quad (7)$$

in which ρ is the density of the crystal, v is an effective velocity of sound, such that

$$v^5=(2/5v_l^5+3/5v_t^5)^{-1},$$

and G_{11} and G_{44} are the spin-phonon coupling coefficients. The anisotropic terms in the relaxation times are, from (6) and (7), proportional to $\frac{9}{16}G_{11}^2-G_{44}^2$; both the degree and sign of the anisotropy depend on the relative sizes of $|3G_{11}/4|$ and $|G_{44}|$. If we define an "anisotropy factor" in terms of the relaxation times for a magnetic field along the [001] and [111] directions by

$$A=[t_1(111)-t_1(001)]/\tfrac{1}{2}[t_1(111)+t_1(001)],$$

then we find that for τ_a, the relaxation time observed after saturation at exact resonance,

$$A_a=(x-1)/\{\tfrac{11}{6}x+1\},$$

where x is $(3G_{11}/4G_{44})^2$. Correspondingly for τ_b,

$$A_b=(1-x).$$

These results assume that the phonon density of states is reasonably isotropic. If it is not, the effective value of x should be altered to take account of the lower (cubic) symmetry of the actual distribution.

In Tables I and II we give the predicted relaxation rates at 4.2°K for H along the [001] direction and the anisotropy factors. The anisotropy factors use the mean of the Watkins-Feher[40] and Shiren[41] results. The experimental values are also shown, and are derived from measurements like those in Fig. 4,

MgO:Fe^{2+}

Here the theoretical predictions are largely confirmed. Thus τ_a is less than τ_b (although the predicted ratio is rather larger than that observed) and the magnitudes of both times are in very reasonable agreement with experiment. The anisotropy has been measured and is in accord with the predictions. In the case of τ_b, if we can neglect other relaxation mechanisms, the anisotropy gives a rather accurate measure of G_{11}/G_{44}, because reasonably large errors in A_b do not introduce corresponding errors in the ratio. We find

$$|G_{11}/G_{44}|=1.59\pm0.09.$$

The error quoted is simply that of the experimental technique. It does not, for example, make any allowance

TABLE I. Spin-lattice relaxation times at 4.2°K with **H** along the [001] axis. We quote t_1T in seconds °K.

	Fe^{2+} Experiment	Fe^{2+} Theory	Ni^{2+} Experiment	Ni^{2+} Theory
τ_aT	1.0×10^{-4}	0.72×10^{-4}	2.6×10^{-3}	8.9×10^{-3} [a]
τ_bT	2.6×10^{-4}	4.5×10^{-4}	3.4×10^{-3}	4.3×10^{-2} [a]

[a] Using the coupling coefficients of Ref. 41 alone.

TABLE II. Anisotropy factors.

	Fe^{2+} Experiment	Fe^{2+} Theory	Ni^{2+} Experiment	Ni^{2+} Theory
A_a	-0.03 ± 0.1	$+0.1$	0.07 ± 0.1	$+0.02$
A_b	-0.4 ± 0.1	-0.38	0.05 ± 0.1	-0.06

[38] J. B. Jones and M. F. Lewis, Solid State Commun. **5**, 595 (1967).

[39] There is an error in Ref. 37 in that the implicit frequency dependence of the $X[2, (200), 2, (200), \alpha, 1, 1]$ coefficients is neglected in the discussion of their Eq. (42). This has been corrected in our expressions.

[40] G. D. Watkins and E. Feher, Bull. Am. Phys. Soc. **7**, 29 (1962).

[41] N. Shiren, Bull. Am. Phys. Soc. **7**, 29 (1962).

for the possibility that we may be measuring a mixture of τ_a and τ_b. Our feeling is that we have measured τ_b by itself, although it is possible that in attempting to measure τ_a, a certain amount of the longer time τ_b may have been admixed. This is because of the experimental difficulties of working exactly at the center of a very wide line, and the admixture would account for both the discrepancy between the predicted and observed values of τ_a/τ_b and for the slight deviations of the anisotropy of τ_a from the predictions.

The absolute magnitudes of $\tau_a T$ and $\tau_b T$ differ slightly from the predictions. The discrepancy, some 40%, could be interpreted as arising from errors in the coupling coefficients or in the assumptions about the phonon system. On the other hand, it may represent some other relaxation mechanism; if it does the estimate of G_{11}/G_{44} will be still less reliable.

$MgO:Ni^{2+}$

There is a pronounced discrepancy between the magnitude of the relaxation rate observed and theoretical estimates. Qualitatively, a number of features of the theoretical model are realized—the isotropy, temperature dependence, and the difference in relaxation rate on and off resonance. However, the *absolute* relaxation rates observed are too fast. This is true even when we consider the specimen which gives the longest relaxation times (we make the usual interpretation of relaxation via fast relaxing impurities in explaining variations of factors of 2 or 3 from sample to sample). It is not the first time that discrepancies have been found between observed rates and those obtained from calculation using experimental coupling coefficients.[42] If we are observing relaxation by impurities, then the temperature dependence (τT constant) shows that the rate determining process is the transfer of energy from the impurity to the lattice, so that the anisotropy observed is that of the impurity relaxation. If we are in fact observing direct relaxation Ni^{2+} to the lattice (which we doubt), then the observed anisotropy would suggest $|G_{11}/G_{44}|=1.33\pm0.08$ and would, in fact, be in agreement with the previous observed values. This estimate of G_{11}/G_{44} will not be used again in this article.

5. THE SATURATION BEHAVIOR

In this section we show that the saturation observed and the rise times, both described in Sec. 3, are consistent with the estimated ultrasonic power level.

The microwave phonons induce $\Delta S_z=\pm1$ transitions in the spin system. The ultrasonic field is pulsed; for simplicity we assume square-wave pulses of duration τ. We define W_p as the probability per unit time that a particular spin makes a transition $\Delta S_z=+1$ due to the ultrasonic pulse. The pulse was applied some distance (typically of the order of 10 spin-packet widths) from the center of the resonance line. As discussed in the last section, two groups of spins will be affected: Those for which the transitions between $S_z=0$ and $S_z=-1$ are induced, and those for which the transitions between $S_z=0$ and $S_z=+1$ are induced. We can treat these groups separately. For the first group, the rate equations are a simple extension of Eqs. (3). If N_i is the number of spins per unit volume in state $S_z=i$, we have

$$\begin{aligned}(d/dt)N_1&=-N_1(\tilde{W}_2+\tilde{W}_3)+N_0W_2+N_{-1}W_3,\\(d/dt)N_0&=N_1\tilde{W}_2-N_0(\tilde{W}_1+W_2+W_p)\\&\qquad+N_{-1}(W_1+W_p),\\(d/dt)N_{-1}&=N_1\tilde{W}_3+N_0(\tilde{W}_1+W_p)\\&\qquad-N_{-1}(W_3+W_1+W_p).\end{aligned}\tag{8}$$

The monitoring spin resonance line had the same frequency as the ultrasonic pulse, and the spin resonance signal measured $n=N_{-1}-N_0$ as a function of the ultrasonic power.

The second and third of Eqs. (8) can be written in the form

$$dn/dt=[\text{thermally induced terms}]-2W_pn.\tag{9}$$

The thermally induced terms vanish at equilibrium when W_p is zero. If the spin system is initially in equilibrium the pulse will cause saturation with a characteristic rise time of the order of $1/2W_p$. The degree of saturation achieved will be close to the equilibrium value if the risetime is appreciably less than the pulse duration τ. The condition that some saturation is observed is, of course, weaker, and we will return to this later. We define the degree of saturation S for the steady state in the presence of the ultrasonic field by

$$n(W_p)=n(W_p=0)[1+S(W_p)]^{-1}.\tag{10}$$

Direct solution of the equations of motion show

$$S\simeq W_p\tau_b[(1+W_1/W_3)/(1+W_1/3W_3)],\tag{11}$$

where τ_b is $1/3W_1$. As W_1/W_3 is small $S\sim W_p\tau_b$. The degree of saturation can be calculated directly. It is independent of the magnitudes of the coupling coefficients G_{11} and G_{44} although it depends on their ratio. We can express $W_p\tau_b$ in the following form, using the results of (6) and (7):

$$W_p\tau_b=\frac{2}{9\pi}\frac{u^2}{v_l^2}\frac{\epsilon_{\text{pulse}}}{\epsilon_{\text{thermal}}}\left\{\frac{\sin^2\theta\cos^2\theta}{(4G_{44}/3G_{11})^2+\sin^2\theta\cos^2\theta+\frac{1}{2}\sin^2\theta}\right\}.\tag{12}$$

This is valid for longitudinal ultrasonic waves propagating along the [001] axis and for spins whose resonant frequency exactly coincides with the ultrasonic frequency. It also assumes that the spin-phonon line shape for each spin packet is Lorentzian with full width at

[42] P. L. Donoho and T. D. Black, in Proceedings of the Fourteenth Colloque Ampere, Ljubljana, 1966 (North-Holland Publihsing Company, Amsterdam, (to be published).

half-intensity Δ, where Δ is much larger than any spread of frequencies in the pulse. u^2 is

$$\frac{1/3v_l^3+2/3v_t^3}{2/5v_t^5}$$

and θ is the angle between the magnetic field [constrained to the $(1\bar{1}0)$ plane] and the crystal [001] axis.

$\epsilon_{\text{thermal}}$ in (12) is the thermal energy per unit volume in a band of width Δ at frequency $\hbar\omega_0$. As $\Delta\sim 6$ Mc/sec we find, in the Debye approximation,

$$\epsilon_{\text{thermal}}\sim 2\times 10^{-5}\ \text{ergs/cc} \tag{13}$$

at 4.2°K. This is uncertain to perhaps $\pm 50\%$ because of the difficulties in estimating Δ.

ϵ_{pulse} is the ultrasonic energy per unit volume in the pulse. The total energy in a 1-μsec pulse can be estimated from the input pulse power (typically 10^2 W, although higher powers were used for the line-shape measurements in Fig. 5), the transducer power conversion efficiency of about 10^{-4} (Ref. 43), and the bond efficiency of about 10^{-1}. This energy is distributed over a volume of order (crystal cross section)$\times v_l\times$(pulse duration), about 0.1 cc in our case. Thus the ultrasonic energy per unit volume is

$$\epsilon_{\text{pulse}}\sim 0.1\ \text{erg/cc}. \tag{14}$$

The degree of saturation S and the rise time can now be checked. From (12) we find that $W_p\tau_b(\simeq S)$ is typically of the order of 0.01 $\epsilon_{\text{pulse}}/\epsilon_{\text{thermal}}$. Thus, from (13) and (14), S is of order 50. The high degree of saturation observed is consistent with this value. Further we see that the rise time $1/2W_p$ will be rather less than 1 μsec, again in agreement with experiment. Peak driving powers in excess of 10^2 W were used when particularly strong saturation was desirable.

This discussion neglects two important features. The first is that, in assuming W_p to be independent of time, we have neglected the attenuation of the pulse as it saturates the spin system. For the Fe^{2+} concentrations in our samples ($\sim$100 ppm) the energy required to saturate the spin packet, starting from 4.2°K, is about 10% of the energy in the ultrasonic pulse. This value is consistent with the power level needed to give appreciable saturation, and serves as a check of our estimates of the various energies. We have also neglected effects arising from the coherence of the microwave ultrasonic field. Experimentally this seems justified; presumably the finite pulse length, the finite transit time through the crystal, and the considerable attenuation are sufficient to eliminate these complications from coherence. Effects such as the inversion of the populations of the energy levels by a 180° pulse could occur in principle (see Ref. 36).

In addition to checking the magnitudes of S and the rise time we can also check the angular dependence of W_p. For longitudinal phonons propagating along the [001] axis the predicted dependence is[8]

$$W_p\sim\sin^2\theta\cos^2\theta, \tag{15}$$

where θ is the angle between the magnetic field and the [001] axis. The observed dependence, shown in Fig. 6, bears a qualitative resemblance to (15). Thus the observed transition probability has a maximum near $\theta=45°$ and has two minima, roughly equal, at $\theta=0°$ and $\theta=90°$. The maximum is reduced because the pulse has been heavily attenuated in partially saturating the spin system. The real difference is the large background, which is roughly independent of θ. One possible explanation is that some of the spins experience an effective magnetic field whose direction differs from that of the applied field because of nearby magnetic ions. Bolef and Gosser[4] observed a similar background in the ultrasonic attenuation and found it to increase rapidly with Fe^{2+} concentration, which would support this explanation. However, if this is so, an appreciable attenuation background should accompany the background saturation in our experiments. This is not observed, and suggests that the longitudinal waves of the main pulse are not responsible for the background saturation.

Several spurious effects could cause some background saturation. For example, transverse waves may be generated accidentally in the transducer,[44] there may be leakage of microwave power between the cavities, or dielectric losses in the quartz transducer may generate a heat pulse. These explanations can be ruled out because the delay between the production of the pulse and the rise in saturation would be different for these mechanisms and the one we have been discussing, and/or because they should persist when the ESR spectrometer is detuned with respect to the ultrasound. Similarly reconversion of ultrasound to microwaves at the quartz/MgO interface can be ruled out by calculation, or because the microwaves would easily be detected if of sufficient intensity to saturate the spins. The most plausible explanation of the background appears to be ultrasonic mode conversion, which has been proposed before[45] to explain a similar background in cw ultrasonic saturation experiments in ruby. The surprising feature of our experiments is that the background is so large—more than 10% of the energy is converted in a single traversal of the MgO. It is not clear if the mode conversion takes place within the MgO or at the surfaces; Tucker's work[45] on Al_2O_3 demonstrated conversion at the surface.

MgO:Fe^{2+} is ideal for the observation of paramagnetic saturation by pulsed phonons because of its strong spin-lattice coupling. Saturation results can be used to estimate spin-lattice coupling coefficients of other systems or to measure the ultrasonic attenuation

[43] H. E. Bommel and K. Dransfeld, Phys. Rev. **117**, 1245 (1960).

[44] The accidental generation of transverse waves in an X-cut transducer can be eliminated by evaporating a metallic film on to the quartz; this shorts out any electric field in the y-z plane.

[45] E. B. Tucker, Proc. IEEE **53**, 1547 (1965).

in the quartz. For both these cases the spin-lattice interaction must be strong enough to give a rise time shorter than, say, the separation of the ultrasonic echoes (about 10 μsec in our experiments). The saturation method has advantages over steady-state saturation techniques in these cases, simply because it is easier to estimate W_p from the energy in each pulse than to estimate the mean-square strain in the steady state from rough values of the phonon lifetimes and input power. The restrictions on the rise time limit the application of the present method. MgO:Ni^{2+} is another system which could be used; we estimate the rise time to be 5–10 μsec in this case.

Some saturation will be observed even in systems with weak spin-lattice coupling. The successive pulses and their echoes induce saturation which accumulates, the degree of saturation reaching a limit which is roughly the cw value reduced by the fraction of the total time for which the spins are exposed to a phonon pulse. We have observed a signal from MgO:Fe^{3+} which was probably taken in these circumstances. This is shown in Fig. 5(c); the magnetic field is along the [111] axis where the lines are sharpest and the spin-lattice interaction close to its maximum. It was not possible to measure the rise time because the Fe^{3+} lines overlap the tail of the Fe^{2+} line.

6. THE SPIN-RESONANCE LINE SHAPES

Several workers have considered the possibility that the widths of the paramagnetic resonance lines in MgO may be caused by internal strains.[28,46,47] These workers have usually assumed some distribution in magnitude for the strains and confirmed that various features of the line shapes are consistent with the same distribution of strains. Thus McMahon[46] found that the $\Delta M=1$, $\Delta M=2$, and double quantum transitions of MgO:Fe^{2+} were strain broadened. Elsa Feher[47] showed that consistent strain distributions could explain the linewidths of MgO:Mn^{2+} and MgO:Fe^{3+} and the angular dependence of the width for these systems.

The choice of a qualitative form for the distribution of strains has been made in several ways. McMahon assumed a Lorentzian distribution because the MgO:Fe^{2+} line shape was very closely Lorentzian. Feher assumed a Gaussian shape for ease of analysis. Neither distribution is entirely satisfactory for, as we will see later, the observed line shape may lie between these two extremes and appears to depend on the component of strain considered. To obtain more complete agreement with experiment one must presumably make a calculation from first principles and consider the details of the dislocation structure. Some attempt to do this has been made by Stoneham.[28] For present purposes we will find, however, that it is often unnecessary to specify a particular shape.

In a perfect MgO crystal lattice the spin Hamiltonian for Fe^{2+} and Ni^{2+} has the simple form

$$H_0=g\beta\mathbf{H}\cdot\mathbf{S},$$

where g is an isotropic g factor. When there are distortions the spin Hamiltonian contains terms linear in the strain. Equation (2) is, in more detail,

$$H_1=G_{11}[\tfrac{1}{4}(2e_{zz}-e_{xx}-e_{yy})(2S_z^2-S_x^2-S_y^2)+\tfrac{3}{4}(e_{xx}-e_{yy})(S_x^2-S_y^2)]$$
$$+G_{44}[e_{yz}(S_zS_y+S_yS_z)+e_{xz}(S_xS_z+S_zS_x)+e_{xy}(S_yS_x+S_xS_y)]. \quad (16)$$

We adopt the notation of Shiren.[26] The axes x, y, z are the cubic axes of the crystal and $\mathbf{e}$ is the strain tensor. We will ignore terms quadratic in the strain as they are small for $\Delta M=1$ transitions even in the case of MgO:Fe^{2+}; the second-order terms are of great importance for the $\Delta M=2$ and double quantum transitions. This perturbation H_1 gives a strain-induced zero-field splitting; it shifts the $S_z=0$ level relative to the $S_z=\pm1$ levels without affecting the separation of the $S_z=\pm1$ levels.

First, the qualitative line shapes are considered. We have studied the line shapes for the magnetic field in the $(1\bar{1}0)$ plane. When the field is at an angle θ from the [001] axis in this plane the transition energies for the two $\Delta M=1$ transitions at a spin where the strain tensor is $\mathbf{e}$ are

$$\hbar\omega=g\beta H\pm\hbar\Delta\omega$$

where

$$\hbar\Delta\omega=G_{11}[\tfrac{1}{2}(3\cos^2\theta-1)][e_{zz}-\tfrac{1}{2}(e_{xx}+e_{yy})]$$
$$+G_{44}[e_{xy}\sin^2\theta+\sqrt{2}\sin\theta\cos\theta(e_{yz}+e_{zx})]. \quad (17)$$

The two cases of particular interest are those when $\mathbf{H}$ is along the cubic [001] axis, when

$$\hbar\Delta\omega=G_{11}(e_{zz}-\tfrac{1}{2}[e_{xx}+e_{yy}]) \quad (18)$$

and when $\mathbf{H}$ is along the trigonal [111] axis ($\cos\theta=1/\sqrt{3}$),

$$\hbar\Delta\omega=\tfrac{2}{3}G_{44}(e_{xy}+e_{yz}+e_{zx}). \quad (19)$$

In the first case only tetragonal strains (and their corresponding coupling coefficient) appear; in the second case only trigonal strains occur.

If the distribution of $[e_{zz}-\frac{1}{2}(e_{xx}+e_{yy})]$ has a full width at half-intensity ϵ_E, the observed spin-resonance line with $\mathbf{H}$ along a cubic axis will have a similar distribution but with width $G_{11}\epsilon_E$. Similarly, when $\mathbf{H}$ lies

[46] D. H. McMahon, Phys. Rev. **134**, A128 (1964).
[47] E. R. Feher, Phys. Rev. **136**, A145 (1964).

along a trigonal [111] axis the spin-resonance line will have width $G_{44}\epsilon_T$, where ϵ_T is the width of the distribution of $\frac{2}{3}(e_{xy}+e_{yz}+e_{zx})$. For reference we compare our notation with that of Ref. 28

$$\epsilon_E \equiv \tfrac{1}{2}\epsilon_{001}; \qquad \epsilon_T \equiv \tfrac{4}{3}\epsilon_{111}.$$

The linewidths quoted in Table III and our previous estimate of $G_{11}(Fe^{2+}) = (1.59\pm0.09)G_{44}(Fe^{2+})$ may be combined to give

$$\epsilon_{100}/\epsilon_{111} = 3.3\pm0.3$$

compared with the theoretical value of 2.3 for an isotropic homogeneous dislocation distribution.[28]

We have so far said nothing about the shape of the resonance line and the strain distribution. There is no need to be explicit for most of what we have to say. The relations between the width of the spin-resonance line and the width of the strain distribution

$$\hbar\Delta\omega_{001} = G_{11}\epsilon_E,$$
$$\hbar\Delta\omega_{111} = G_{44}\epsilon_T \qquad (20)$$

hold irrespective of the detailed shape. They also hold if we use, instead of the full widths at half-intensity of the distributions, the separation of the points at which the derivatives of the distributions are largest. In fact we are only concerned about the shape of the strain distribution in two situations. The first is when we want to compare the distribution with theory, that is, when we are interested in the shape *per se*. The second is when we want to extract the strain contribution to the linewidth from other effects, such as dipolar broadening. For present purposes, the assumption of a Lorentzian shape is sufficiently good for the dipolar contribution about 2 G wide to be subtracted.

The observed resonance lines are nearly Lorentzian. Their shape is, however, dependent on the direction of the magnetic field, and is narrower in the wings for **H** along [111] than when **H** lies along the cubic axis. The only prediction appears to be that of Stoneham,[28] who obtained a line shape

$$I(\omega) = 2\pi^{-1}\int_{-\infty}^{\infty} dx \exp[i(\omega-\omega_0)x] \times \exp[-x^2(A-B\ln|x|)] \qquad (21)$$

in which A and B depend on the relevant components of strain, the density of dislocations, and the Burgers vectors. If B were zero, this would be a Gaussian shape; when B is finite the intensity is even lower in the wings than for a Gaussian distribution. The conflict between the predicted shape and experiment was discussed in Ref. 28 and is almost certainly a result of the neglect of the subgrain structure of the dislocation distribution in MgO crystals. The main point of interest here is, however, that the ratio B/A depends on which components of **e** are considered. In particular B/A will differ for the distribution of $e_{zz}-\frac{1}{2}(e_{xx}+e_{yy})$ and of $(e_{xy}+e_{zx}+e_{yz})$, so the line shapes for **H** along [001] and for **H** along [111] should be different. Detailed calculation shows that the predicted shape should fall off slightly faster in the wings for **H** along the [111] axis than for the field along a cube axis. This is observed. It is not clear how seriously one should treat the agreement, for an especially simple dislocation distribution is assumed and subgrain structure neglected. What is encouraging is that the simple model does predict a dependence of the line shape on field direction qualitatively similar to that observed.

TABLE III. Linewidths in Oe. The separation of the points of maximum slope of the various lines are given. The three widths for Mn^{2+} and Fe^{3+} are for the $(-\frac{1}{2}\rightarrow\frac{1}{2})$, $(\frac{1}{2}\rightarrow\frac{3}{2})$, and $(\frac{3}{2}\rightarrow\frac{5}{2})$ lines, respectively; for these systems the errors are estimated to be between 5 and 7%.

	Ion	⟨100⟩ field	⟨111⟩ field
Crystal I	Fe^{2+}	634±12	322±6
	Fe^{3+}	0.95, 12, 21	1.0, 2.1, 3.2
	Mn^{2+}	0.85, 3, 5.7	0.8, 1.2, 1.8
Crystal II	Ni^{2+}	50±2	35±2
	Fe^{3+}	1.1, 8.9, 17	1.2, 2.05, 3.1
	Mn^{2+}	0.95, 2.5, 4.5	1.15, 1.4, 1.8

We may use the strain-broadened contributions to the observed linewidths, $\Delta\omega_{100}$ and $\Delta\omega_{111}$, with Eqs. (20) to compare coupling coefficients (G_{11} and G_{44}) and the strain fields in which ions of different species occur. Experimentally, we obtain the product of a coupling coefficient and a parameter of the strain distribution, e.g., $G_{11}\epsilon_E$ or $G_{44}\epsilon_T$. These data will now be used to compare the magnitude of coupling coefficients.

If the coupling coefficients are known from static-stress measurements[40] or from ultrasonic attenuation work[41] the strain distributions experienced by different ions may be compared. It appears that different spins (say Ni^{2+} or Fe^{2+}) experience essentially identical distributions of strains. This seems to hold as accurately as experimental errors allow; in particular, the agreement between strain distributions from different species is at least as good as that between strain distributions from different transitions of the same species (see, for example, McMahon's work on MgO:Fe^{2+} and the work on MgO:Co^{2+} cited in Table I of Ref. 28). From this we may conclude first that there is no appreciable tendency for the spins considered to accumulate near to the dislocations—there is no correlation in space between the spins and the sources of strain. Secondly, the properties of the individual ions do not significantly affect the strain distribution. This means that the ions considered do not show a static Jahn-Teller distortion of more than the detection limit of about 0.3×10^{-4}; some of the ions should definitely not show a distortion (e.g., the S-state ions Mn^{2+} and Fe^{3+}) whereas others (notably Fe^{2+} and Ni^{2+}) could in principle, show a distortion.

Instead of assuming values for the coupling coefficients and deducing strain distributions we may assume all species experience the same distribution of strains and compare the magnitudes of the coupling coefficients. This is analogous to a static-stress experiment except that the dislocations in the crystal provide the stresses and the strength of the stress must thus be found from the effect on the linewidth of some other spin in the crystal. Also as strains of both signs occur it is not possible to obtain the *signs* of the coupling coefficients. However we should be able to improve the consistency of the various sets of coupling coefficients obtained by other workers. The reason that we are able to do this is that the method of measuring line shapes (by saturating with phonons when it is necessary to get a zero line) is remarkably sensitive, whereas straight ESR measurements are rather crude in the case of very broad lines.

The three cases on which we concentrate are those of Fe^{2+}, Fe^{3+}, and Ni^{2+} in MgO. Our final accuracy has been limited by the fact that it has not been possible to grow crystals with appreciable amounts of both Ni^{2+} and Fe^{2+}. Consequently we have compared the widths of the Fe^{3+} and Ni^{2+} lines in one crystal to obtain the $G_{ij}(Fe^{3+})/G_{ij}(Ni^{2+})$ and we have compared the Fe^{2+} and Fe^{3+} linewidths in a second crystal to obtain the $G_{ij}(Fe^{3+})/G_{ij}(Fe^{2+})$. The ultimate accuracy is limited by the extent to which we can separate the strain-broadening and dipolar broadening contributions to the Fe^{3+} width. Other errors, such as in the actual measurements of the linewidths and in the contributions of dipolar broadening to the broad Fe^{2+} and Ni^{2+} lines, are relatively small. We also used the Mn^{2+} linewidths as well as the Fe^{3+} to check our work. The two contributions to the Fe^{3+} line shape are separated by noting that the dipolar contribution should be independent of the transition considered, whereas the inhomogeneously broadened contribution to the different transitions $(\frac{5}{2}\cdot\frac{3}{2})$, $(\frac{3}{2}:\frac{1}{2})$, and $(\frac{1}{2}:-\frac{1}{2})$, should be in the ratio 2:1:0. The resulting line shapes are, of course, the convolutions of these two contributions, at least in the reasonable approximation that there is no correlation between the defects causing dipolar broadening and those which introduce the inhomogeneous strain broadening.[28] If both the contributions were Lorentzian the resulting width would be the sum of the component widths

$$\Delta H=\Delta H_{\rm dip}+\Delta H_{\rm inh}. \tag{22}$$

On the other hand, if both components were Gaussian (as assumed by Feher) then

$$\Delta H=[(\Delta H_{\rm dip})^2+(\Delta H_{\rm inh})^2]^{1/2}. \tag{23}$$

Both the observed line shapes and theoretical arguments favor (22), and this equation gives a more consistent set of values for $\Delta H_{\rm inh}$. The linewidths are given in Table III. From these we deduce

$$|\,G_{11}(Fe^{2+})/G_{11}(Ni^{2+})\,|=10.0\pm0.2 \tag{24}$$

compared with Shiren's 11 ± 4 and the Watkins-Feher value 14 ± 4. For the trigonal coupling coefficients

$$|\,G_{44}(Fe^{2+})/G_{44}(Ni^{2+})\,|=7.8\pm0.8, \tag{25}$$

where the accuracy is reduced by the difficulty of separating the dipolar contribution to the Fe^{3+} and Mn^{2+} widths. Shiren's value for (25) is 7.6 ± 3, and that of Watkins and Feher is 15 ± 4. Clearly these *ratios* are in slightly better agreement with Shiren's estimates.

Finally, we use the ratios (24) and (25), together with $|\,G_{11}(Fe^{2+})/G_{44}(Fe^{2+})\,|$ obtained in Sec. 4 to derive a "consistent" set of coupling coefficients for Ni^{2+} and Fe^{2+}. In doing so it should be emphasized that (24) and (25) assume that all ions in MgO experience the same internal strain field. Further, the estimate

$$|\,G_{11}(Fe^{2+})/G_{44}(Fe^{2+})\,|=1.59\pm0.09 \tag{26}$$

assumes that the MgO phonon system is essentially isotropic and that no unexpected relaxation mechanisms affect the degree of anisotropy of the relaxation. Although (24), (25), and (26) establish the *ratios* of the coupling coefficients quite well, the *magnitude* of one of the coefficients must be chosen in some way from absolute measurements, such as those of Refs. 40 or 41. For example, if we choose $G_{44}(Fe^{2+})=\gamma$ then we have

$$G_{11}(Fe^{2+})=(1.59\pm0.09)\gamma,$$
$$G_{44}(Fe^{2+})=\gamma,$$
$$G_{11}(Ni^{2+})=(0.159\pm0.012)\gamma,$$
$$G_{44}(Ni^{2+})=(0.128\pm0.012)\gamma.$$

There is no obvious way of choosing γ. One possibility would be to equate the *product* of these four coefficients with the corresponding experimental values. We then find $\gamma=407$ from the data of Ref. 40 and $\gamma=384$ from that of Ref. 41. The former estimate may be more reliable as coupling coefficients obtained from static-stress measurements are not liable to the systematic errors inherent in concentration measurements. With this value,

$$G_{11}(Fe^{2+})=647\pm40,$$
$$G_{44}(Fe^{2+})=407,$$
$$G_{11}(Ni^{2+})=64.7\pm6,$$
$$G_{44}(Ni^{2+})=52.0\pm5.$$

Systematic errors in γ, possibly as high as 50%, are not included.

Our discussion so far has been confined to the $\Delta M=1$ line, which corresponds to an allowed transition in both acoustic and conventional spin resonance. As the line is strongly inhomogeneously broadened the acoustic

and ESR line shapes should be essentially identical (for dipolar broadening this is not necessarily the case; this is discussed in Refs. 48–51). The $\Delta M=2$ lines have, however, quite different shapes in acoustic and conventional resonance. This can be seen by comparing Fig. 5(d), where the acoustic line shape is given with Fig. 5(c) which gives the usual ESR line shape. Figure 5(d) was obtained using piezo electric measurement of the echo height at low phonon powers. Although one cannot draw quantitative conclusions from it because of phase cancellation effects (most important at high phonon powers[52,53]), it is clear that the $\Delta M=2$ line shape is not identical with that in Fig. 5(c). The phonon line shape [Fig. 5(d)] is enhanced on the low-field side relative to the (conventional) photon line shape of Fig. 5(c). The explanation, due to Rampton[54] is this. The $\Delta M=2$ line is allowed for phonons because of their quadrupolar selection rule,[55] but forbidden for the photons which have dipolar selection rule if the Fe^{2+} are in a cubic crystal field. The departures from cubic symmetry reinstate the (photon) ESR line with a transition probability which is greatest for ions in the most distorted sites—i.e., for the ions whose contributions to the $\Delta M=2$ line occur at the lowest fields. This explanation accounts for two observations previously reported by one of us (M.F.L.). In Ref. 17 it was stated that the ultrasonic attenuation drops faster than the ESR line shape on the low-field side of the $\Delta M=2$ line. In Ref. 16 it was noted that the ultrasonic attenuation and dispersion were *not* greatest where the ESR signal was a maximum; this was wrongly attributed to a second ultrasonic attenuation mechanism.

7. CONCLUSION

We have examined the saturation behavior of MgO:Fe^{2+} and the spin-resonance line shapes and spin-lattice relaxation times for Ni^{2+} and Fe^{2+} in MgO. The saturation behavior is quantitatively consistent with theory, although the angular dependence of the transition probability W_p deduced from the saturation has a background attributed to ultrasonic mode conversion. The spin-lattice relaxation times of Fe^{2+} are in good agreement with theory in magnitude, in dependence on the magnetic field orientation and in their dependence on the position of measurement in the inhomogeneous line. Under the rather drastic assumptions that the lattice is dynamically isotropic[56] and that no other relaxation mechanisms complicate the direct process relaxation, the anisotropy of the relaxation rate gives $|G_{11}(Fe^{2+})/G_{44}(Fe^{2+})|=1.59\pm0.09$. The agreement of theory and experiment for Ni^{2+} is less satisfactory, possibly due to the presence of fast relaxing impurities.

The saturation by ultrasonics has been exploited to measure the Fe^{2+} line shape with considerably greater accuracy that conventional methods allow. The most interesting qualitative result is that the line shape changes with magnetic field orientation. This is in qualitative agreement with theoretical work on strain broadening by dislocations.[28] The angular dependence of the linewidth is also obtained, and we find $\epsilon_{001}/\epsilon_{111}=3.3\pm0.3$; this is in acceptable agreement with the approximate theoretical value of 2.3. Further by comparing the linewidths of Fe^{2+} and Ni^{2+} and by making the assumption that the ions in MgO all experience the same internal strain distribution we find

$$|G_{11}(Fe^{2+})/G_{11}(Ni^{2+})|=10.0\pm0.2$$

and

$$|G_{44}(Fe^{2+})/G_{44}(Ni^{2+})|=7.8\pm0.8.$$

The quoted errors are considerably less than those in the ratios of coupling coefficients measured more directly. It is possible to use these ratios to improve the consistency of the coupling coefficients already published, but it is difficult to choose an absolute magnitude for the set of coefficients because of systematic errors in the published measurements.

[48] R. Loudon, Phys. Rev. **119**, 919 (1960).
[49] A. M. Stoneham, Phys. Letters **14**, 297 (1965).
[50] K. W. H. Stevens and J. W. Tucker, Phys. Letters **14**, 291 (1965).
[51] A. M. Stoneham, Phys. Letters **18**, 22 (1965).
[52] V. W. Rampton and P. M. Rowell, J. Phys. Chem. Solids **28**, 395 (1961).
[53] H. M. Rosenberg, J. K. Wigmore, and M. F. Lewis, Phil. Mag. **15**, 701 (1967).
[54] V. W. Rampton, Ph.D. thesis, University of Nottingham, England, 1965 (unpublished).
[55] R. D. Mattuck and M. W. P. Strandberg, Phys. Rev. **119**, 1204 (1960).
[56] It may be worth commenting that C. F. Weissfloch [Can. J. Phys. **44**, 2509 (1966)] has shown that the elastic anisotropy of Al_2O_3 does not significantly affect the orientation dependence of the relaxation rate of $Al_2O_3:Cr^{3+}$.

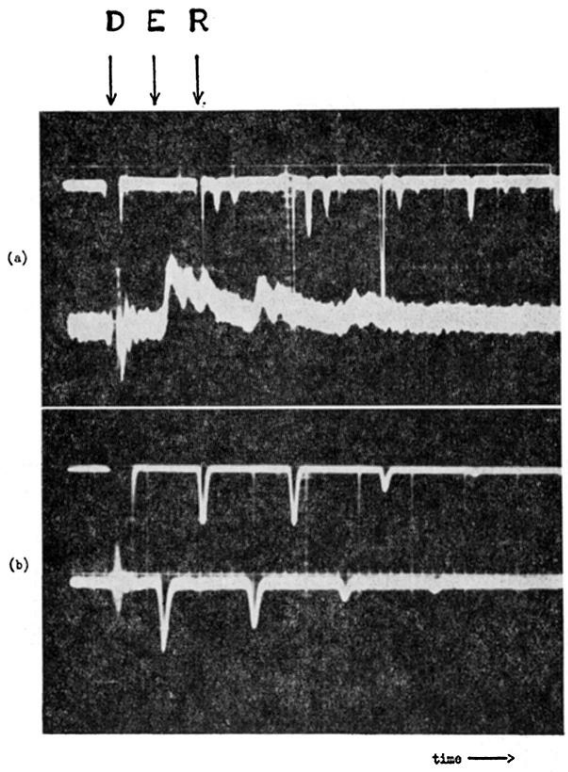

FIG. 3. Echo patterns detected piezoelectrically (upper traces) and saturation signals (lower traces) at 4.2°K. The large scale divisions of the time base are 5 μsec apart. D is the driving pulse, E the point at which the phonon pulse enters the MgO, and R the first reflection from the MgO: quartz bond. (a) MgO with about 100 ppm Fe^{2+}; only about one-third of the MgO specimen is in the ESR cavity. (b) MgO with about 3000 ppm Fe^{2+}. All the specimen is in the ESR cavity. The opposite signs of the lower (saturation) traces in (a) and (b) are of no significance. The first echo of the lower trace in (b) is slightly reduced by electronic effects.